corrosion and materials degradation

MDPI

Article

Development of an Optimized NDT Methodology for the Investigation of Ancient Greek Copper-Based Artifacts

Amani-Christiana Saint, Vasiliki Dritsa and Maria Koui *

NDT Laboratory, Materials Science and Engineering Section, School of Chemical Engineering, National Technical University of Athens, 9, Iroon Polytechniou Street, Zografou, 15773 Athens, Greece; amani45@gmail.com (A.-C.S.); vdritsa@mail.ntua.gr (V.D.)

* Correspondence: markoue@chemeng.ntua.gr; Tel.: +30-2107723214

Abstract: A multi-analytical non-destructive testing (NDT) methodology was applied to copper-based artifacts originated from various archaeological sites of Greece. X-ray fluorescence (XRF), fiber optics diffuse reflectance spectroscopy (FORS) and scanning electron microscopy coupled with an energy dispersive X-ray detector (ESEM-EDX) were used for the characterization of the alloys and the corrosion products. The key elements of the artifacts belonging to the Early Bronze Age (2700–2300 BC) were copper and arsenic, while tin bronze was used for the fabrication of the Late Bronze Age (1600–1100 BC) artifacts. The effectiveness of XRF for the determination of the bulk composition was confirmed by comparative study with the previously applied atomic absorption spectroscopy (AAS) and inductively coupled plasma–atomic emission spectrometry (ICP-AES) destructive techniques. Significant differences between the artifacts were revealed through the spectral measurement of their surface corrosion products color by FORS. ESEM-EDX provided information on the microstructure, the elemental composition of the corrosion layers and bulk, as well as the distribution of the corrosion products on the surface. Conclusively, the combined NDT methodology could be regarded as a valuable and appropriate tool for the elemental composition of the bulk alloy, thus leading to the classification of their historical period and the corrosion products, contributing significantly to their conservation–restoration.

Keywords: XRF spectroscopy; FORS; ESEM-EDX; arsenical copper; tin bronze; corrosion; alloy composition; Late Bronze Age; Early Bronze Age

Citation: Saint, A.-C.; Dritsa, V.; Koui, M. Development of an Optimized NDT Methodology for the Investigation of Ancient Greek Copper-Based Artifacts. *Corros. Mater. Degrad.* **2021**, *2*, 325–340. https://doi.org/10.3390/cmd2020017

Academic Editor: José Inácio Ferrão de Paiva Martins

Received: 30 March 2021
Accepted: 9 June 2021
Published: 15 June 2021

1. Introduction

Copper was the first metal used and dates back at least ten thousand years B.C. The first evidence for the exploitation of copper ore comes from the region of Anatolia and Iran, where copper objects date from the 9th to the 7th millennium B.C. During the 4th millennium B.C., the practice of alloying became widely known and used during the Early Bronze Age (EBA), unlike the earlier Copper Age (or Chalcolithic period), when copper (Cu) predominated in metalworking [1–3].

In Greece, alloying Cu with arsenic (As) begins during the Late Neolithic and the Early Bronze Age (EBA), significantly enhancing the workability. Arsenical copper was used in all parts of ancient Greece and mainly in the Aegean region. Following the arsenical copper, arsenical bronze (as an intermediate step) and then bronze (Cu-Sn alloy) emerged during the Late Bronze Age (LBA), although low (about 1–3 wt%) tin (Sn) alloys can be found in all civilizations and might have been accidentally produced by natural tin bronze deposits. However, bronzes containing Sn in a higher concentration (above 5 wt%) are mostly deliberate alloys by the addition of cassiterite (SnO_2) to molten copper [4].

The investigation of historic copper-based artifacts, of various historical periods and origins, has been the objective of numerous research studies. During the past years, the destructive techniques of atomic absorption spectroscopy (AAS) [4–14] and inductively coupled plasma–atomic emission spectrometry (ICP-AES) [14–17] predominated for the

determination of the bulk chemical composition of historic artifacts. In addition, research is also focused on the characterization of the surface corrosion products and the investigation of their formation mechanism [18–22], via the employment of several different techniques, either alone or combined. Patinas can provide valuable indications for the composition of the bulk, since the nature of the corrosion products that are formed on their surface is differentiated depending on the nature of the alloy used, museum conditions and the burial environment and the species of the environment (moisture, air, pH, ions concentration, soil composition, presence of microorganisms, objects of different composition buried in the same place, etc.). Additional information that can be derived includes their historical period, their place of origin but also their burial environment through the identification of the physicochemical processes that took place during their corrosion [23,24].

However, the great archaeological and artistic value of historic copper-based artifacts results in the restriction or even the prohibition of sampling, settling the need for the employment of non-destructive testing (NDT) techniques.

In the present work, a multi-analytical NDT methodology consisting of in situ XRF and FORS was used for the investigation of 32 copper-based artifacts dated at the Early Bronze Age (2700–2300 BC) and the Late Bronze Age (1600–1100 BC). The combined methodology of portable XRF and FORS was applied to multiple spots of the corroded surface of the objects. A small-size fragment of the object No 10816 was analyzed using the ESEM-EDX technique for the microstructure investigation and the analysis of the bulk and the surface corrosion products chemical elemental composition. ESEM-EDX was used in a completely non-destructive manner for the investigation of copper alloy patina and the integrity of the object itself was not affected by the analysis being performed. The quantitative results of XRF analysis were compared with detailed bulk composition analysis obtained by destructive laboratory techniques in order to assess the accuracy and reliability of XRF analysis in corroded surfaces. The bulk composition of the former objects has been determined in the past by means of AAS (performed in the Chemical and Physical Research Department of the National Archaeological Museum of Athens) and ICP-AES (performed in the Chemical Engineering School of National Technical University of Athens) techniques [4,12,15,17].

2. Materials and Methods

2.1. Copper-Based Artifacts

The studied 32 artifacts consist of several types of copper-based tools, such as chisels, double axe, saw, razor, weapons such as swords, daggers, tableware such as bowls, basin, as well as a significant number of copper fragments. The artifacts originated from various archaeological sites of Greece and belong to the Prehistoric Collection of the National Archaeological Museum of Athens, Greece. A total of 19 copper-based chisels originated from Macedonia, Petralona, and dated at the EBA II (2700–2300 BC) have been examined. The chisels belong to the so-called "Petralona hoard". The term "hoard" is used to describe a deliberately gathered and hidden group of precious objects during troubled times [13]. All chisels were cast in an open mold and then finished by hammering. The investigated one-handled bowl, a luxury object of its time (object No. 10816), was found in numerous fragments, being part of the Mycenaean "Andronianoi hoard", which consists of 9 artifacts, discovered in Andronianoi, Euboea, Greece, and dated at the LBA (1600–1100 BC), specifically to the Late Helladic IIB period (1450–1400 BC). The group from Andronianoi is probably to be assigned to the active scene of metalworking and commercial exchanges of the wider region and the nearby harbor of Kyme, as a hoard for exchange during 1500–1300 BC [25]. Apart from the bowl, 8 copper-based objects of "Andronianoi hoard" such as a saw, double axe, daggers, swords, razor and spearhead were investigated. Among the studied artifacts, two Naue II swords of unknown provenance (Nos. 9885 and 13905), a bowl (No. 11934) and a large basin (No. 11949) from Peloponnese, Argolid, dated back at the LBA (14th–12th Century BC) were also analyzed. The term "Naue II" sword type is believed to be of west European origin and was introduced into the Aegean by way of the Adriatic in the second

half of the 13th century BC. During the 12th BC the swords, now of local manufacture, were widely distributed in the Greek Mainland especially in Achaea, Peloponnese and also found in Cyclades, Dodecanese, Crete.

The objects, dated at the Early and Late Bronze Age are shown in Figures 1–3, respectively.

Figure 1. 19 Chisels originated from Macedonia, Chalkidiki, Petralona, and dated at the Early Bronze Age (2700–2300 BC) —Nos. 17794–17812.

Figure 2. Nine copper-based objects (a saw, a double axe, daggers, swords, a razor, a spearhead and a bowl in fragments) originated from Euboea—the "Andronianoi hoard"—Nos. 10797, 10798, 10810–10816, dated back at the LBA (15th–12th century BC).

Figure 3. Copper-based Naue II swords of unknown provenance (Nos. 9885 and 13905), a bowl (No. 11934) and a large basin (No. 11949) from Peloponnese, Argolid, dated back at the LBA (14th–12th century BC).

2.2. XRF Spectroscopy

A portable XRF Tracer III-SD (Bruker-AXS, Madison, WI, USA) was employed for the in situ, non-destructive chemical elemental composition analysis of the artifacts. The spectrometer is equipped with a rhodium tube from which X-rays are emitted and a Peltier-cooled, silicon PIN diode detector, operating at 40 kV and 15 μA from an external power source. Each spectrum was received for 200 live seconds with the use of a filter composed of 1 mil titanium (Ti) and 12 mil aluminum (Al). The setting of the X-ray tube eliminates the Rh L to assure that the trace elements can be detected in the raw spectrum. The fluorescence signal derives from about 0.1 mm depth of a copper alloy. The Bruker ARTAX software (v. 5.3.0.0) was used for qualitative data analysis for all elements present calculated. ARTAX uses an automated process, which involves the deconvolution and evaluation of the spectra, including background and escape corrections. Data were then processed using S1CalProcess with empirical calibrations to produce wt% elemental compositions.

2.3. Vis-NearIR FORS

In situ measurements were performed on the corroded surfaces of the selected copper-based objects, in multiple spots, using a portable Ocean Optics, USB4000-VIS-NIR Fiber Optic Reflectance Spectrometer (FORS, Ocean optics, Dunedin, FL, USA). The instrument features a high-performance 3648-element linear CCD-array detector, installed with a multi-band pass order-sorting filter to cover the 350–1000 nm wavelength range and a 25 μm entrance slit for optical resolution to 1.5 nm. The instrument is equipped with

a QR400-7-VIS/NIR reflection bifurcated probe providing illumination and detection of diffused light form the same direction, an HL-2000 tungsten- halogen light source and a probe holder positioning the QR400-7 at 45° for diffuse reflection in order not to include specular reflectance. Use of this device also allows one to guarantee a correct contact with the surface to be analyzed, to keep constant the sample-to-probe distance (about 4 mm), at the same time avoiding external light contributions. Diffuse reflectance spectra were referenced against WS-1 Diffuse Reflectance Standard, provided by Ocean Optics and guaranteed reflective at 98 wt% or more in the spectral range investigated. Diffuse reflectance spectra were recorded in the range of 350–1000 nm. Spectral data treatment was performed with the Spectrasuite software® (Ocean Optics) add-on for Excel/Origin.

2.4. ESEM-EDX

A small fragment of the selected copper-based object No. 10816 (Figure 2) dated at the LBA was examined by means of ESEM-EDX for the microstructure investigation and the analysis of the bulk and the surface corrosion products chemical elemental composition. A FEI Quanta 200 Environmental Scanning Electron Microscope (ESEM), coupled with an Energy Dispersive X-Ray detector (EDX) was used. During the microstructure analysis, three types of images were shown by the respective detectors: (a) the secondary electron (SE) by the Everhart–Thomley detector (ETD), depicting morphology, (b) the back scattered electron (BSE) by the Solid State Electron Detector (SSD), showing phase distributions and (c) a mixed picture (mix) which was a digital combination of the former images. The fragment was mounted on a carbon tab to the sample holder. SEM imaging parameters, selected based on overall quality of the image were as follows: 30 kV accelerating voltage, magnifications up to 12,000× and detector dead time of 5 μs for each single image. The surface and the bulk elemental composition (in cross-section) were determined by the EDX detector using spot analysis locally at different selected spots of special interest and surface analysis (mapping) on the whole image. High resolution images were obtained without gold or carbon coating, thereby enabling imaging of the sample close to its original state, without requiring any pretreatment.

3. Results

3.1. XRF Results

XRF analysis was applied on the surface of the copper-based artifacts. In order to minimize the effect of corrosion, ten measurements on different areas of the object were conducted and the mean value was taken as a final value. Representative XRF spectra of an EBA Object No. 17805 and LBA Object 10812 are shown in Figure 4. The results obtained from the EBA chisels (Table 1) revealed that Cu is the main element (concentration varied from 86.66 to 96.04 wt%). Moreover, the high concentration of As ranging from 1.1 to 2.6 wt% is indicative of an copper-arsenic alloy [26].

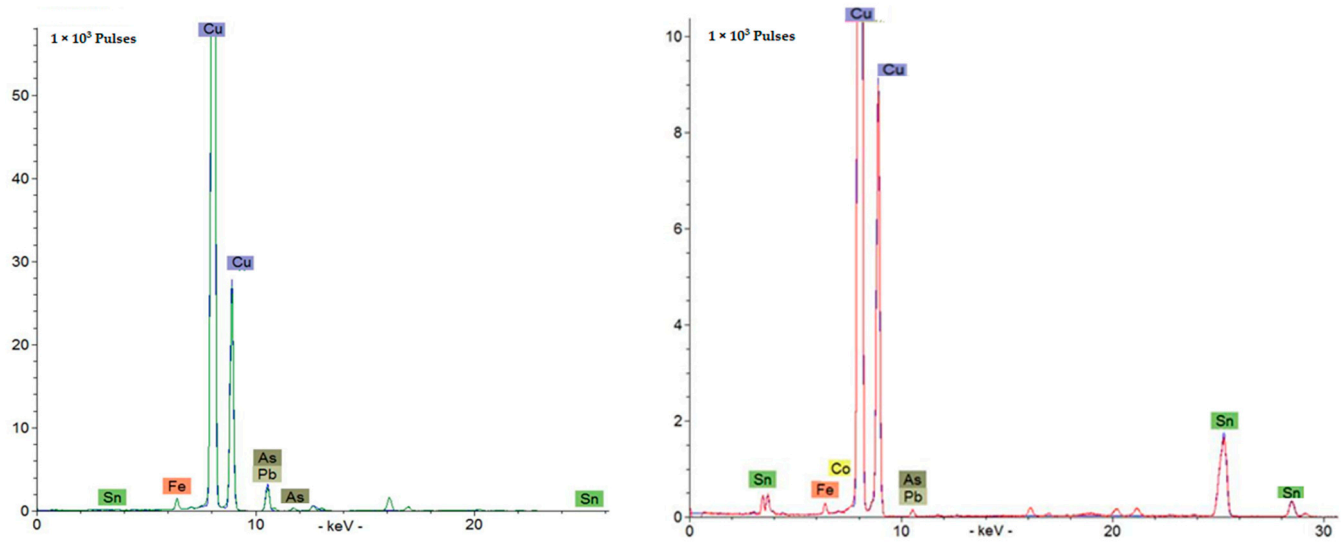

(**a**) (**b**)

Figure 4. XRF spectrum of copper-based (**a**) Object No. 17805 dated at the Early Bronze Age; (**b**) Object 10812 dated at the Late Bronze Age.

Table 1. Chemical composition (wt%) determined by XRF spectrometry of the copper-based objects Nos. 17794–17812, Early Bronze Age (2700–2300 BC).

No	Cu	As	Bi	Ni	Co	Ag	Zn	Sn	Pb	Sb	Fe
17794	90.91	1.93	0.26	n.d.	n.d.	0.15	0.06	0.12	n.d.	0.13	2.88
17795	91.00	1.98	1.44	n.d.	n.d.	0.09	0.05	0.04	n.d.	0.12	1.38
17796	93.18	2.31	1.03	0.04	n.d.	0.07	0.07	0.12	n.d.	0.17	1.18
17797	90.50	2.12	1.65	n.d.	n.d.	0.20	0.06	0.06	n.d.	0.19	2.22
17798	88.81	2.03	0.64	n.d.	n.d.	0.05	0.05	0.06	n.d.	0.19	3.69
17799	86.66	2.61	1.06	n.d.	n.d.	0.01	n.d.	0.02	n.d.	0.14	0.78
17800	93.72	1.26	0.61	n.d.	n.d.	0.09	0.07	0.02	n.d.	0.10	1.48
17801	94.85	1.71	0.88	0.02	n.d.	0.13	0.08	0.02	n.d.	0.08	0.35
17802	95.42	1.61	0.29	n.d.	n.d.	0.09	0.08	0.02	n.d.	0.22	n.d.
17803	92.79	1.96	0.45	0.08	n.d.	0.08	0.05	0.05	n.d.	0.11	0.86
17804	87.23	1.72	0.84	n.d.	n.d.	0.11	0.01	0.04	1.232	0.13	1.55
17805	94.92	1.390	0.80	0.03	0.01	0.10	0.15	0.02	1.750	0.07	0.29
17806	96.04	1.200	0.46	0.02	n.d.	0.13	0.10	0.40	n.d.	0.13	0.29
17807	94.31	2.338	0.22	0.16	n.d.	0.10	0.08	0.09	n.d.	0.15	0.59
17808	93.30	1.913	0.80	0.15	n.d.	0.08	0.09	0.12	n.d.	0.18	1.03
17809	91.28	1.486	0.29	n.d.	n.d.	0.15	0.10	0.18	n.d.	0.18	2.56
17810	91.52	1.299	0.08	n.d.	n.d.	0.27	0.10	0.19	n.d.	0.13	2.74
17811	91.69	1.131	0.22	n.d.	n.d.	0.16	0.11	0.18	n.d.	0.26	2.74
17812	92.37	2.159	1.06	0.04	n.d.	0.14	0.08	0.13	n.d.	0.13	0.70

n.d. = not detected.

The mechanical properties of copper change significantly by increased concentration of As (>0.5 wt%), which enhances cold work hardness and castability and decreases the melting point of copper. High concentration of Bi was also detected (0.08–1.65 wt%), indicating that it is a part of the copper ore [27]. Lead (Pb) was detected only in two objects (No. 17804 and 17805) with an average concentration of 1.23 and 1.75 wt%, respectively (Figure 4). In addition, the main elements, Ni, Co, Ag, Zn, Sn, Pb and Sb, were detected in traces, or not detected at all. Ag, Zn, Sn and Sb contents are less than 0.5 wt% in all objects, so they should be regarded as minor elements. In most samples, the high Fe content ranging from 0.35 to 3.7 wt% may be attributed to remains from the surrounding

environment, deposited on their surface, since the examined Early Bronze Age objects have not been submitted to any cleaning treatment.

The elemental composition of the Late Bronze Age artifacts is shown in Table 2. The elemental composition of the Late Bronze Age artifacts (Table 2) determined by XRF analysis showed that the objects are generally characterized by high purity tin-bronze alloys with 5.54 to 18.84 wt% Sn content and low presence of impurities, independently from their provenance and typology. The average concentration of Cu is around 86 wt% (standard deviation 3.3) and Sn average concentration is around 12 wt% (standard deviation 3.5), as a major component of the alloy of the LBA artifacts, contrary to the EBA objects for which Sn is an impurity. The different amount of tin used in the objects, which may be attributed to tin's availability in an area or the absence of a standardized alloying practice. The elements As, Ni, Co, Ag, Zn, Pb, Sb, Fe and Bi were detected in low concentrations. The examined LBA copper-based objects have been submitted to mechanical cleaning of their surfaces thus, lower Fe concentrations are detected, compared to the EBA artifacts.

Table 2. Chemical composition (wt%) determined by XRF spectrometry of the copper-based objects Nos. 10797, 10798, 10810–10816, 9885, 13905, 11934, 11949, Late Bronze Age (1600–1100 BC).

No	Cu	Sn	As	Ni	Co	Ag	Zn	Pb	Sb	Fe	Bi
10797	85.81	12.49	0.11	n.d.	n.d.	n.d.	0.15	n.d.	0.02	0.91	0.03
10798	84.24	14.15	0.11	n.d.	0.001	0.03	0.25	0.19	0.12	0.32	0.10
10810	84.44	15.21	0.34	0.11	0.02	n.d.	0.35	0.13	0.04	0.11	0.08
10811	88.21	11.85	0.11	n.d.	n.d.	n.d.	0.12	n.d.	0.05	0.15	0.02
10812	84.98	14.82	0.01	n.d.	n.d.	n.d.	0.12	0.04	n.d.	0.37	0.02
10813	82.95	15.88	0.11	n.d.	0.001	n.d.	0.28	0.26	0.14	0.33	0.15
10814	79.87	18.84	0.25	n.d.	n.d.	n.d.	0.20	n.d.	0.09	0.56	0.10
10815	83.27	10.85	0.60	n.d.	0.05	n.d.	3.17	0.09	0.03	0.38	0.01
10816	86.97	9.31	0.39	n.d.	0.02	n.d.	2.49	n.d.	0.004	0.08	0.01
9885	92.10	5.80	0.12	n.d.	0.01	n.d.	0.10	n.d.	0.03	0.87	0.01
2740	90.21	6.45	0.19	1.19	0.25	0.12	0.51	0.06	n.d.	0.05	0.04
2539	94.63	1.16	0.28	1.28	0.09	0.07	0.89	n.d.	n.d.	0.03	0.04
1017	80.80	10.98	5.90	1.61	0.29	0.21	0.06	0.02	0.02	0.05	0.11
10185	89.79	9.12	0.06	0.23	0.20	0.15	0.30	0.04	0.09	0.01	n.d.
10186	86.79	10.91	0.77	0.68	0.64	0.12	0.10	0.06	0.04	0.02	n.d.
13905	89.65	9.04	0.19	0.07	0.02	0.01	0.11	0.13	0.11	0.29	0.05
11934	86.53	12.70	0.10	n.d.	n.d.	n.d.	0.10	n.d.	0.03	0.51	0.04
11949	90.03	9.81	0.01	n.d.	n.d.	0.01	0.11	0.06	0.06	0.17	0.03

n.d. = not detected.

The XRF results for the Early Bronze Age artifacts are in good agreement with the AAS analysis results [25]. Similar compositions were determined for most of the examined elements. In particular, Cu concentrations ranging from 85.45 to 89.39 wt%, a considerable As content around 2 wt% and low presence of impurities were determined. Fe concentrations are significantly different due to the fact that AAS samples were taken from the bulk of the objects, resulting also to limited differentiations concerning the other elemental contents. Further differences may be attributed to the method limitations or to corrosion process.

The results from XRF analysis for the LBA objects are also in good agreement with the respective AAS and ICP-AES analysis results that showed high Sn contents ranging from 5.94 to 14.07 wt% [25]. The contents of the characteristic elements Cu and Sn were similar without significant differences, apart from the object No. 10816. However, the AAS analysis for the object No. 10186 was not accurate as the total content in not 100%.

3.2. In Situ FORS Results

VIS-NIR FORS analysis was performed in situ on the green corroded surfaces of the copper-based objects. FORS analysis indicated significant differences in Figure 5 between the Early Bronze Age (a) and the Late Bronze Age (b) objects reflectance spectra, especially regarding the maximum wavelength of the diffuse reflectance curve and reflectance intensity.

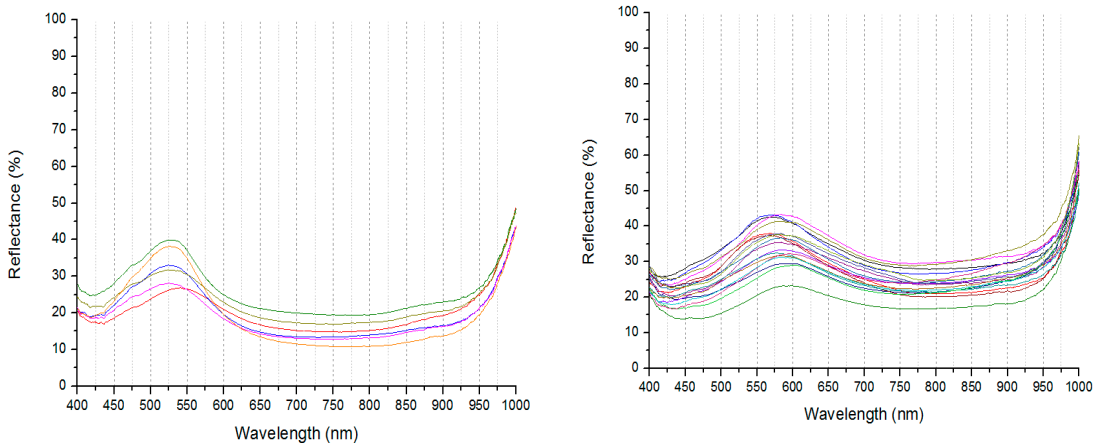

Figure 5. Diffuse reflectance spectra indicating differences regarding the reflectance maximum position and the reflectance intensity: (**a**) Late Bronze Age copper-based objects; (**b**) Early Bronze Age copper-based objects.

In particular, the spectra from the LBA objects (Cu-Sn alloy) exhibit a reflectance maximum in wavelengths varying between 530–550 nm. Concerning the spectra from the EBA artifacts (Cu-As alloy), a shift of the maximum in higher wavelengths varying between 550–590 nm (with the majority of collected spectra to exhibit a maximum near 570 nm) is observed, which could be due to the different bulk alloy composition between the Early and the Late Bronze Age objects, which results in the formation of different corrosion products and, as a consequence, in different color. The presence of malachite could be identified through the spectra of the LBA objects, indicated by the broad absorption band appearing near 770 nm [28–30].

3.3. ESEM-EDX Results

At a small fragment of the artifact No. 10816, extensive chemical elemental analysis was performed on the corroded surface and in cross-section, by means of ESEM-EDX in the laboratory. A part of the corroded surface of the fragment is shown in Figure 6a, magnified by 200×. Brighter spots correspond to concentrated Ag (back scattered electron image). In the total area, the EDX analysis reveals that the predominant elements are O, C and Cu. Moreover, considerable concentrations of Ca, Cl, Si and Ag are determined in Table 3. In the same region, magnification by 6000× revealed a needle-shaped formation rich in Ag, as it is shown in the EDX elemental analysis of the spot in Figure 6b. Representative EDX elemental analysis results at multiple spots and areas of the corroded surface of the fragment are reported in Table 3.

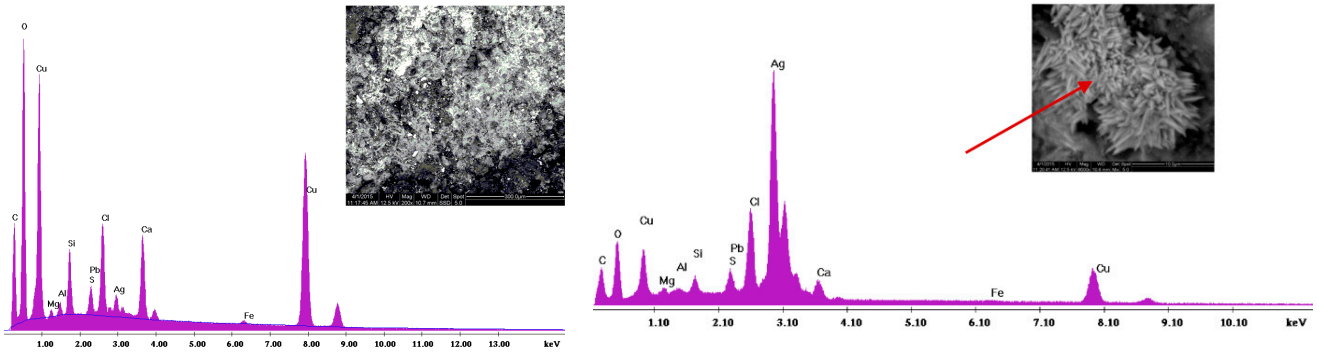

(**a**) (**b**)

Figure 6. SEM image and EDX analysis: (**a**) Corroded surface magnified by 200×—Area 1, the presence of Ag corresponds to the brighter spots; (**b**) A needle-shaped formation on the corroded surface magnified by 6000× and elemental analysis spectrum of the spot—Spot 1 (red arrow).

Table 3. EDX chemical elemental analysis of the corroded surface of a fragment of the artifact No. 10816 at multiple spots and areas (wt%).

Element	Area 1 Mapping (200×)	Spot 1 (6000×)	Area 2 Mapping (200×)	Area 3 Mapping (400×)
O	40.30	25.08	28.65	24.01
C	23.41	13.74	20.58	25.67
Cu	20.72	28.54	39.10	39.48
Ca	3.81	2.25	2.28	1.40
Cl	3.72	1.98	3.56	3.26
Si	2.82	1.85	2.19	2.10
Ag	2.53	22.12	1.66	3.21
S	1.45	3.46	0.97	0.54
Al	0.59	0.41	0.48	0.32
Mg	0.45	0.44	0.33	-
Fe	0.21	0.12	0.22	-
Pb	n.d.	n.d.	n.d.	n.d.
Sum.	100.0	100.0	100.00	100.00

n.d. = not detected.

Elements O, C and Cu are also detected, while S is present in considerable concentration. The concentration/distribution of various elements, alone or combined, overlaid with the respective area of the SE image in Figure 7a, magnified 400×, corresponding to the investigated surface of the full mapping (Area 3, Table 3) are depicted in Figure 7b–l.

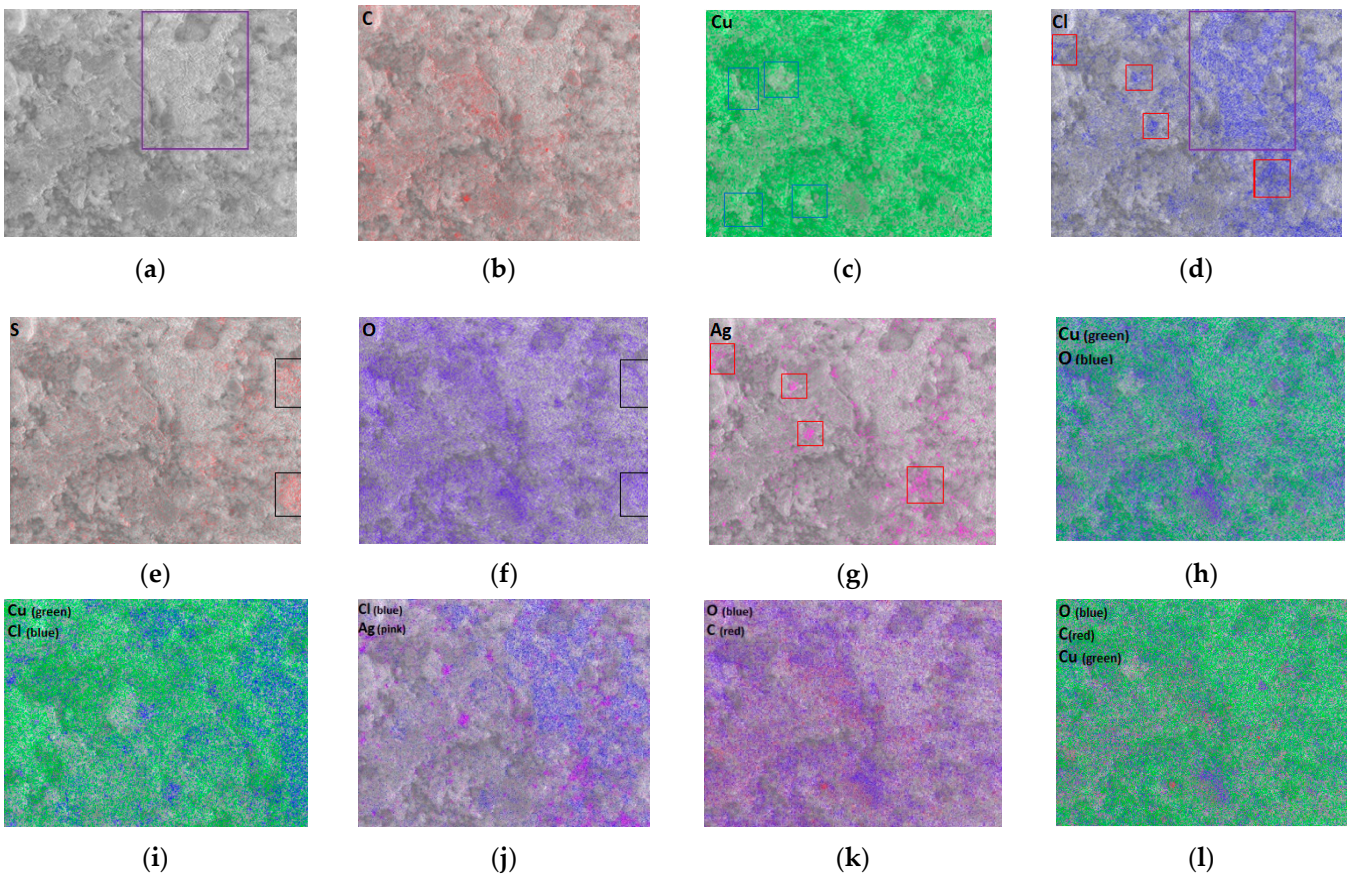

Figure 7. (**a**) Corroded surface, magnification 400×; (**b**) Concentration of C; (**c**) Concentration of Cu; (**d**) Concentration of Cl; (**e**) Concentration of S; (**f**) Concentration of O; (**g**) Concentration of Ag, (**h**) Concentration of Cu (green) and O (blue); (**i**) Concentration of Cu (green) and Cl (blue); (**j**) Concentration of Cl (blue) and Ag (pink); (**k**) Concentration of O (blue) and C (red); (**l**) Concentration of O (blue), C (red) and Cu (green).

As it is shown in Figure 7d, in a particular area of the investigated surface, Cl is highly concentrated. Chlorine-based compounds endanger the integrity of a bronze object, as they lead to copper degradation. In particular, Cl- anions from the burial soil react with Cu forming CuCl and can undergo redox reactions with oxygen and moisture leading to copper degradation phenomenon (bronze disease). This reaction affects remarkably the chemical-physical stability of the alloy and is destructive, transforming the bronze in a greenish powder [31]. As it is observed in Figure 7i, elemental Cl coincides with Cu in some spots, probably forming $CuCl_2$ or a basic copper chloride $Cu_2(OH)_3Cl$ [19,30]. In Figure 7d,g,j, Cl coincides with Ag, probably forming AgCl. Chlorides are characteristic corrosion products formed in historic copper-based objects buried in areas with high levels of NaCl, possibly close to marine or submarine areas [30]. Areas with high S concentrations in Figure 7e seem to overlap with high concentration of O, indicating the presence of sulfur oxides and copper sulfides in the corroded surface. Figure 7h reveals that Cu and O can be extensively found combined; thus, copper oxides or hydroxides may be present. It is well-known that in Cu-Sn alloys, in case of soil burial environment, the surface corrosion layer is constituted of Cu (II) salts, such as malachite ($Cu_2(CO_3)(OH)_2$), which presents a green hue, (or other salts for the air and sea-water exposed objects) [19]. This is further confirmed in Figure 7k,l by the superficial color of the examined object. It is reported that this outer corrosion layer covers a cuprous oxide layer in contact with the metal core [19]. Al and Si are closely detected thus, silicon oxides are most probably present. It is confirmed that the presence of hydroxysilicates together with silica or aluminosilicates from the soil, are typical compounds of the outer corrosion layer in Cu-Sn alloys [19].

The morphology of the surface of the fragment in cross section is shown in Figure 8a. At the area depicted in Figure 8b, including only the bulk surface of the fragment, EDX analysis revealed significant differences in composition compared to the corroded surface. The concentrations of C and O were significantly reduced and Cu concentration was increased, compared to the EDX analyses of the corroded surface, due to the fact that this surface was not oxidized to an extended degree.

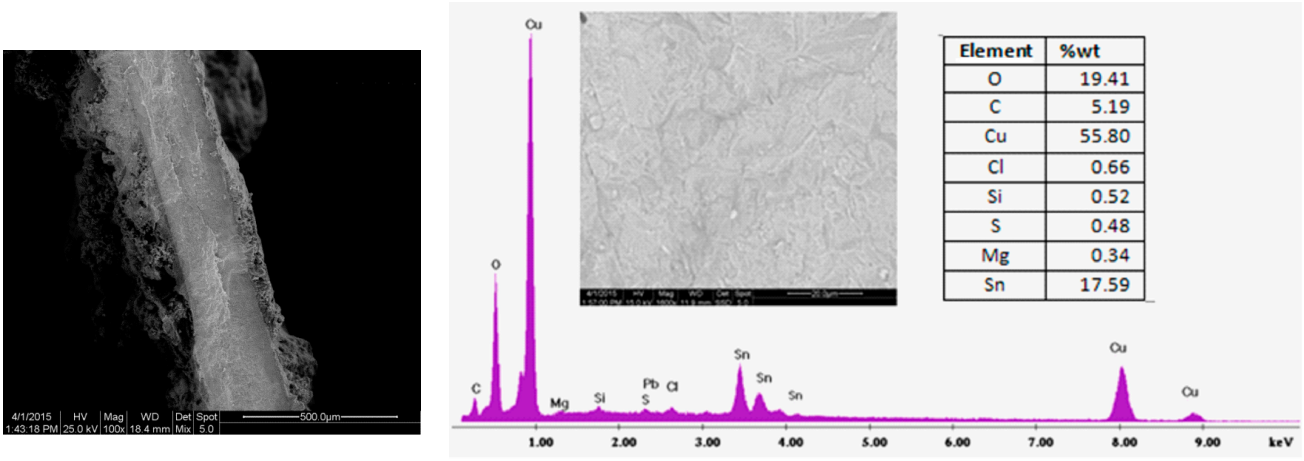

(**a**) (**b**)

Figure 8. SEM image of the cross-section of the fragment No. 10816: (**a**) Magnification 100×; (**b**) Magnification 1600× and EDX analysis.

Furthermore, Sn is additionally presented, as part of the Cu-Sn alloy of the LBA artifact, which was not detected in the EDX analyses of the corroded surface. On the contrary, through the XRF measurements on the corroded surface, Sn was identified, as the XRF presents a higher penetration depth compared to the ESEM-EDX. Moreover, Cl and Si concentrations are decreased, while Al was not detectable, compared to the results obtained from the corroded surface investigated. The absence of Ag is also noticeable, as this element was identified in the corroded surface (mostly on spot analyses) and was also detected by means of AAS in a concentration of 0.2% in the bulk of the object. Ca was not detected, confirming that its presence is due to a burial environment deposit [19,30]. A full mapping of the area of the bulk and corroded surface (cross-section) was performed in order to determine the areas where each element is distributed, as it is shown in Figure 9a. In Figure 9b, the positions of each element concentration/distribution on the area are investigated. The parallel lines set the limits of the bulk of the sample. It is indicated that Cu presents a higher concentration in the bulk surface and it is also detected at the corroded surfaces. C is mostly concentrated at the corroded surfaces. O is dispersed at the whole surface, but it presents higher concentration at the corroded surfaces. Finally, Sn is concentrated in the bulk surface of the fragment.

The occurrence of elements such as Si, Al, S, O and Cl only in the corrosion layers/areas and not in the bulk of the tin bronze artifact can be referred to oxidation while buried in soil, which led to the formation of secondary corrosion products (oxy-hydroxides, silicates, chlorides, sulfates and carbonates) [19,23,30,32–37].

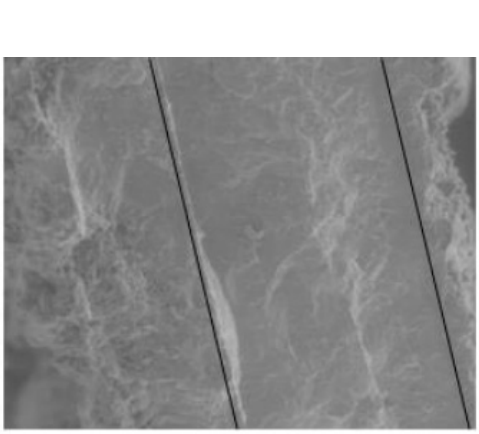

Element	%wt
O	20.87
C	16.52
Cu	49.39
Cl	0.97
Si	3.34
Ag	0.18
S	0.44
Al	0.17
Pb	0.17
Sn	7.95

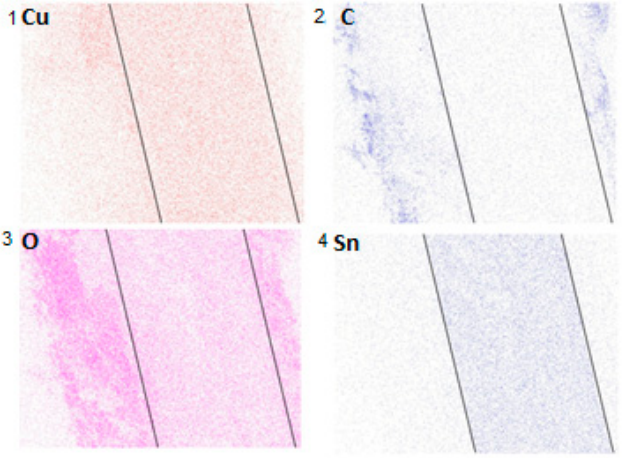

(**a**) (**b**)

Figure 9. (**a**) SEM image and EDX analysis (600×) of the surface (corroded and bulk); (**b**) Concentration of Cu (**1**), C (**2**), O (**3**), Sn (**4**).

4. Discussion

A collection of 32 copper -based artifacts was investigated with the use of a combined NDT methodology for the chemical characterization of the bulk and corrosion products. XRF analysis was applied on the surface of the copper-based artifacts in order to yield qualitative and quantitative information regarding the chemical elemental composition, enabling the characterization of the metal or metal alloy, the identification of the historical period of copper-based artifacts through evidence of key-elements, also having the potential to relate metal compositions to ore deposits through their minor element pattern. The accuracy and resolution of the XRF analysis was confirmed by comparing the acquired XRF data with the former compositional data, obtained by means of and ICP-AES, as mentioned above. XRF analysis enabled the identification of major and minor elements of the Early and Late Bronze Age artifacts and allowed the determination of the key-elements. Apart from the main element Cu, As and Bi were detected in the artifacts from for the Early Bronze Age. Cu and Sn were identified in the objects dated at the Late Bronze Age. The elemental characterization of the alloys (Cu-As and Cu-Sn) became the determinant factors in the classification of the copper-based objects into two different historical periods. The high concentration of As is indicative of a copper-arsenic alloy which provides the alloy with upgraded mechanical properties. An increased concentration of As (>0.5 wt%) enhances cold work hardness and castability and decreases the melting point of copper [26]. Due to the geological co-occurrence of arsenic and copper minerals as well as the smelting of such polymetallic ores for the production of arsenical copper, it has not been established if arsenical copper alloys were deliberately or intentionally created [38]. The presence of Pb can be considered as random and it is probably related to the impurities of particular copper ores used for the fabrication of these alloys or providing a clue for the use of recycled metals [39]. The high Fe content may be attributed to remains from the surrounding environment, deposited on their surface, since the examined Early Bronze Age objects have not been submitted to any cleaning treatment. The chemical characterization of the Late Bronze Age artifacts revealed that they consisted of high purity tin-bronze alloys content and low presence of impurities, independently from their provenance and typology. Due to the mechanical cleaning of their surfaces, lower Fe concentrations were detected, compared to the EBA artifacts.

Although XRF analysis is performed on the corroded surfaces of the artifacts and may alter the determined concentrations of secondary metals, in our case, the accuracy of the XRF analysis was not affected. As a surface technique, XRF analysis is representative for the bulk alloy when the surface is consistent with the underlying metal. Due to its

significant advantage over methods that require sampling and a single analysis may or may not represent the entire object, XRF allows the non-destructive examination of multiple spots. Thus, large scale variations can be identified properly and representative results can be obtained [39]. As a result, in situ XRF technique allows the qualitative and quantitative analysis of the determinant elements that classify the copper-based objects into the specific historical period.

VIS-NIR FORS analysis was performed in situ on the green corroded surfaces of the copper-based objects. FORS is a surface analysis and may allow the chemical and mineralogical characterization of surface corrosion products, based on chemical fingerprints, as well as an approach of the identification of the bulk alloy composition through the spectral measurement of their surface corrosion products color. Significant differences were observed in the maximum wavelength of the diffuse reflectance curve and reflectance intensity differences between the EBA and LBA objects reflectance spectra. The presence of malachite was indicated in LBA objects. Malachite is acknowledged as the most usual corrosion product developed by the corrosion of copper alloys buried in the soil. The first product to be formed, adjacent to the metal surface, is cuprite [28–30].

According to ESEM-EDX analysis, there are three corrosion layers. The outer corrosion layer presents a green hue and consists of alkaline compounds of copper (II) such as hydrocarbons, hydrochlorides, hydroxides and hydrosilicates together with silica or aluminosilicates due to the burial environment. The intermediate layer contains cuprous oxides as well as chloride ions, while the chemical composition of the internal corrosion layer—in contact with the bulk of the object—is characterized by the presence of Cu with O and locally Si, but also Sn and Cl [19,23,30,32–37].

5. Conclusions

Archaeological copper-based artifacts of different historical periods and various origins were studied, via a multi-analytical NDT methodology including portable XRF and FORS. In addition to the former in situ techniques, ESEM-EDX, a laboratory technique, was used in a non-destructive manner, as the integrity of the fragment was not affected. The extensive use of arsenical copper alloys in Early Bronze Age was confirmed due to the determination of copper and arsenic elements by XRF analysis. On the contrary, tin bronze alloys prevailed in Late Bronze Age, as copper and tin were the main elements in the selected copper-based objects. Although XRF technique is performed on the surface, it is well-suited for the identification of the alloys, as the results are in good agreement with the elemental concentration values of previously applied AAS and ICP-AES techniques. Additionally, FORS technique indicates the spectral differences between the Early and the Late Bronze Age objects. ESEM-EDX analysis confirmed the reliability of XRF results and also enabled the differentiation of the surface corrosion products from the elemental composition of the bulk. Conclusively, the combined methodology XRF and FORS could be regarded as a valuable and appropriate non-destructive tool for the identification of the bulk alloy composition of historic copper-based objects, leading to their historical period classification and contributing significantly to their conservation–restoration. The additional application of ESEM-EDX, in case sampling is allowed, can integrate the results concerning the investigation of the corrosion products.

Author Contributions: Investigation, writing—original draft preparation, formal analysis, A.-C.S. and V.D.; methodology, writing—review and editing V.D. and M.K.; supervision, M.K. All authors have read and agreed to the published version of the manuscript.

Funding: This research was co-financed by the European Union (European Social Fund—ESF) and Greek national funds through the Operational Program "Education and Lifelong Learning" of the National Strategic Reference Framework (NSRF), project number MIS: 379472. The Doc-Culture research project THALES entitled "Development of an Integrated Information Environment for assessment and documentation of conservation interventions to cultural works/objects with Non Destructive Techniques (NDTs)", was coordinated and managed by NTUA.

Institutional Review Board Statement: Not applicable.

Informed Consent Statement: Not applicable.

Data Availability Statement: All required data provided in the manuscript.

Acknowledgments: The authors would like to thank the National Archaeological Museum of Athens, Greece and especially the Archeologist Katerina Kostanti for allowing the investigation of the historic artifacts and for the collaboration.

Conflicts of Interest: The authors declare no conflict of interest.

References

1. De Ryck, I.; Adriaens, A.; Adams, F. An overview of Mesopotamian bronze metallurgy during the 3rd millennium BC. *J. Cult. Herit.* **2005**, *6*, 261–268. [CrossRef]
2. Tylecote, R.F. *A History of Metallurgy*, 2nd ed.; Maney Materials Science: London, UK, 1992.
3. Cheilakou, E. The Application of Spectroscopic and Non Destructive Testing & Evaluation Techniques (NDT&E) for the Materials Characterization, the Decay Inspection and the Conservation-Restoration of Historic Artefacts. Ph.D. Thesis, NTUA, School of Chemical Engineering, Materials Science and Engineering Section, Athens, Greece, 2011.
4. Mangou, H.; Ioannou, P.V. On the chemical composition of Prehistoric Greek Copper-Based Artifacts from Mainland Greece. *BSA* **1999**, *94*, 81–100.
5. Pernicka, E.; Begemann, F.; Sphmitt-Stecker, S.; Grimanis, A.P. On the composition of metal artifacts from Poliochni on Lemnos. *Oxf. J. Archaeol.* **1990**, *9*, 263–297. [CrossRef]
6. Mangou, H.; Ioannou, P.V. On the chemical composition of Prehistoric Greek Copper- Based Artifacts from the Aegean Region. *BSA* **1997**, *92*, 59–72.
7. Mangou, H.; Ioannou, P.V. On the chemical composition of Prehistoric Greek Copper- Based Artifacts form Crete. *BSA* **1998**, *93*, 91–102.
8. Stos-Gale, Z.; Sampson, A.; Mangou, E. Analyses of metal artifacts from the Early Helladic Cemetery of Manika on Euboia. *Aegean Archaeol.* **1996**, *3*, 49–62.
9. Gilmore, R.G.; Ottaway, S.B. Micromethods for the Determination of Trace Elements in Copper-based Metal Artifacts. *J. Archaeol. Sci.* **1980**, *7*, 241–254. [CrossRef]
10. Mangou, H.; Ioannou, P.V. Studies of the Late Bronze Age copper-based ingots found in Greece. *BSA* **2000**, *95*, 207–217. [CrossRef]
11. Mangou, H.; Ioannou, P.V. Trends in the making of Greek copper-based artefacts during the prehistoric period (4000-1050 BC). *OpAthRom* **2002**, *27*, 105–118.
12. Andreopoulou-Mangou, E. Chimiki analysi metallikon antikeimenon mykinaikis epochis apo tous Andronianous Evoias. *EAM Mous.* **2005**, *5*, 45–50. (In Greek)
13. Grammenos, D.; Tzachili, I. O thesavros ton Petralonon this Chalkidikis. *Archaeol. Ephemer.* **1994**, *85*. (In Greek)
14. Pernicka, E.; Begemann, F.; Schmitt-Strecker, S.; Todorova, H. KuleffI. Prehistoric copper in Bulgaria, its composition and provenance. *Eurasia Antiq.* **1997**, *3*, 41–180.
15. Koui, M.; Papandreopoulos, P.; Andreopoulou-Mangou, E.; Papazoglou-Manioudaki, E.; Priftaj-Vevecka, A.; Stamati, F. Study of Bronze Age copper based swords of type Naue II and spearheads from Greece and Albania. *Mediterr. Archaeol. Archaeom.* **2006**, *6*, 5–22.
16. Bourgarit, D.; Mille, B. The elemental analysis of ancient copper-based artefatcs by inductively-coupled-plasma atomic-emission spectrometry: An optimized methodology reveals some secrects of the Vix crater. *Meas. Sci. Technol.* **2003**, *14*, 1538–1555. [CrossRef]
17. Koui, M.; Andreopoulou-Mangou, E.; Papazoglou-Manioudaki, E.; Papandreopoulos, P. Preliminary results from the study of the composition ant the Manufacturing technique of Prehistoric Age copper objects from the Greek area. In Proceedings of the 2nd Greek Congress of Metal Materials, Athens, Greece, 25–26 November 2004; pp. 143–150. (In Greek).
18. Mattsson, E.; Nord, A.G.; Tronner, K.; Fjaestad, M.; Laglerlof, A.; Ullen, I.; Borg, G.C. Deterioration of archaeological material in soil-Results on bronze artefacts. In *Konserveringstekniska Studier*; RIK 10; Riksantikvarieambetet: Stockholmm, Sweden, 1996; pp. 16–80.
19. Robbiola, L.; Blengino, J.M.; Fiaud, C. Morphology and mechanisms of formation of natural patinas on archaeological Cu-Sn alloys. *Corros. Sci.* **1998**, *40*, 2083–2111. [CrossRef]
20. Geilmann, W. Verwitterung von Bronzen in Sandboden. Ein Beitrag zu Korrosionsforschung. *Angew. Chem.* **1956**, *68*, 201–211. [CrossRef]
21. Scott, A.D. Periodic corrosion phenomena in bronze antiquities. *Stud. Conserv.* **1985**, *33*, 49–57.
22. Tylecote, R.F. The effect of soil conditions on the long-term corrosion of buried tin-bronzes and copper. *J. Archaeol. Sci.* **1979**, *6*, 345–368. [CrossRef]
23. De Ryck, I.; Pantos, E.; Adriaens, A. Near Eastern ancient bronze objects from Tell Beydar (NE- Syria): Insights into their corrosion. *Eur. News* **2007**, *38*, 29–33. [CrossRef]

24. Constantinides, I.; Adriaens, A.; Adams, F. Surface characterization of artificial corrosion layers on copper alloy reference materials. *Appl. Surf. Sci.* **2002**, *189*, 90–101. [CrossRef]
25. Saint, A.C.; Dritsa, V.; Cheilakou, E.; Koui, M. Non-invasive discrimination of early and late Bronze Age copper-based objects by means of XRF spectroscopy. In Proceedings of the 9th International Symposium on the Conservation of Monuments in the Mediterranean Basin, Ankara, Turkey, 3–5 June 2014; pp. 521–529.
26. Craddock, P. The composition of the copper alloys used by Greek, Etruscan and Roman civilizations: The Greeks before the Archaic Period. *J. Archaeol. Sci.* **1976**, *3*, 93–113. [CrossRef]
27. Hosler, D. *The Sounds and Colors of Power. The Sacred Metallurgical Technology of Ancient West Mexico*; MIT Press: Massachusetts, MA, USA, 1994.
28. Cheilakou, E.; Koui, M. Corrosion products identification of simulated ancient copper alloys and Bronze Age copper based objects by Fiber Optics Diffuse Reflectance Spectroscopy technique (FODRS). In Proceedings of the XIII Balkan Mineral Processing Congress, Bucharest, Romania, 17–19 June 2009; Volume 1, pp. 79–86.
29. Cheilakou, E.; Koui, M. Fiber Optics Diffuse Reflectance Spectroscopy (FODRS) as a tool for the non destructive characterization of ancient copper based artefacts through the measurement of their colour. In Proceedings of the 6th International Conference on Instrumental Methods of Analysis, Athens, Greece, 4–8 October 2009; p. 152.
30. Scott, A.D. Copper and Bronze in Art. In *Corrosion, Colorants, Conservation*; Getty Publications, The Getty Consertion Institute: Los Angeles, CA, USA, 2002.
31. Ingo, G.M.; Riccucci, C.; Giuliani, C.; Faustoferri, A.; Pierigè, I.; Fierro, G.; Pascucci, M.; Albini, M.; Di Carlo, G. Surface studies of patinas and metallurgical features of uncommon high-tin bronze artefacts from the Italic necropolises of ancient Abruzzo (Central Italy). *Appl. Surf. Sci.* **2019**, *470*, 74–83. [CrossRef]
32. De Ryck, I.; Adriaens, A.; Pantos, E.; Adams, F. A comparison of microbeam techniques for the analysis of corroded ancient bronze objects. *Analyst* **2003**, *128*, 1104–1109. [CrossRef]
33. Casaletto, M.P.; Ingo, G.M.; Albini, M.; Lapenna, A.; Pierige, I.; Riccucci, C.; Faraldi, F. An integrated analytical characterization of corrosion products on ornamental objects from the necropolis of Colle Badetta-Tortoreto (Teramo-Italy). *Appl. Phys. A* **2010**, *100*, 801–808. [CrossRef]
34. Ingo, G.M.; de Caro, T.; Riccucci, C.; Angelini, E.; Grassini, S.; Balbi, S.; Bernardini, P.; Salvi, D.; Bousselmi, L.; Çilingiroglu, A.; et al. Large scale investigation of chemical composition, structure and corrosion mechanism of bronze archeological artefacts from Mediterranean basin. *Appl. Phys. A* **2006**, *83*, 513–520. [CrossRef]
35. Oudbashi, O.; Emami, S.M.; Ahmadi, H.; Davami, P. Micro-stratigraphical investigation on corrosion layers in ancient Bronze artefacts by scanning electron microscopy energy dispersive spectrometry and optical microscopy. *Herit. Sci.* **2013**, *1*, 1–10. [CrossRef]
36. He, L.; Liang, J.; Zhao, X.; Jiang, B. Corrosion behavior and morphological features of archeological bronze coins from ancient China. *Microchem. J.* **2011**, *99*, 203–212. [CrossRef]
37. Arafat, A.; Na'es, M.; Kantarelou, V.; Haddada, N.; Giakoumaki, A.; Argyropoulos, V.; Anglos, D.; Karydas, A.G. Combined in situ micro-XRF, LIBS and SEM-EDS analysis of base metal and corrosion products for Islamic copper alloyed artefacts from Umm Qais museum, Jordan. *J. Cult. Herit.* **2013**, *14*, 261–269. [CrossRef]
38. Lechtman, H. Arsenic Bronze: Dirty Copper or Chosen Alloy? A View from the Americas. *J. Field Archaeol.* **1996**, *23*, 477–514.
39. Bottaini, C.; Vilaça, R.; Montero-Ruiz, I.; Mirão, J.; Candeias, A. Archaeometric contribution to the interpretation of the Late Bronze Age "hoard" from Porto Do Concelho (Macão, Central Portugal). *Mediterr. Archaeol. Archaeom.* **2017**, *17*, 217–231.